DALTON
FULL PAPER

A unified mechanism for the stoichiometric reduction of H^+ and C_2H_2 by $[Fe_4S_4(SPh)_4]^{3-}$ in MeCN

Karin L. C. Grönberg, Richard A. Henderson* and Kay E. Oglieve

John Innes Centre, Nitrogen Fixation Laboratory, Norwich Research Park, Colney, Norwich, UK NR4 7UH. E-mail: richard.hendrsn@bbsrc.ac.uk

Received 29th April 1998, Accepted 10th July 1998

The kinetics and mechanisms of the conversions of H^+ into H_2 and C_2H_2 into C_2H_4 by $[Fe_4S_4(SPh)_4]^{3-}$, using $[Hlut]^+$ (lut = 2,6-dimethylpyridine) as the proton source, have been investigated in MeCN. At high concentrations of $[Hlut]^+$, $[Fe_4S_4(SPh)_4]^{3-}$ rapidly binds three protons to give $[Fe_4S_2(SH)_2(SPh)_3(SHPh)]$, and it is only in this protonation state that the cluster is capable of transforming the substrates. Kinetic studies indicated that subsequent dissociation of the thiol from $[Fe_4S_2(SH)_2(SPh)_3(SHPh)]$ to generate $[Fe_4S_2(SH)_2(SPh)_3]$ is also essential for H_2 and C_2H_4 production. It is proposed that the vacant site on one of the Fe atoms allows protonation of this Fe by $[Hlut]^+$ to form $[Fe_4HS_2(SH)_2(SPh)_3]^+$. Reduction of this species by another molecule of reduced cluster {probably $[Fe_4S_2(SH)_2(SPh)_3(SHPh)]$} gives the "super-reduced" cluster $[Fe_4HS_2(SH)_2(SPh)_3]$ {and $[Fe_4S_2(SH)_2(SPh)_3(SHPh)]^+$}. Subsequently the "super-reduced" cluster releases H_2 and produces $[Fe_4S_2(SH)_2(SPh)_3(SHPh)]^+$. In the presence of C_2H_2, $[Fe_4HS_2(SH)_2(SPh)_3]^+$ binds the alkyne to form $[Fe_4HS_2(SH)_2(SPh)_3(C_2H_2)]^+$. Subsequent reduction (as above) produces the "super-reduced" $[Fe_4HS_2(SH)_2(SPh)_3(C_2H_2)]$, then C_2H_4. However, binding C_2H_2 does not completely suppress H_2 formation and $[Fe_4HS_2(SH)_2(SPh)_3(C_2H_2)]$ produces H_2 *ca.* 30% of the time. The results of earlier studies on the reduction of H^+ and C_2H_2 by structurally analogous Fe–S-based clusters are discussed and shown to be consistent with this mechanism.

Introduction

The transformation of small molecules by coupled electron- and proton-transfer reactions is a dominant feature of both chemical and biological catalysis.[1] Conceptually, the simplest such reaction is the reduction of H^+ to H_2 which is accomplished in Nature by both hydrogenases[2] and nitrogenases.[3] In both classes of enzymes the active sites are Fe–S-based clusters. Thus, in the Fe-only hydrogenases this transformation is believed to occur at the (so-called) H-clusters,[4] whose structure has not yet been established by crystallography but a 6Fe6S core has been proposed.[1] In the molybdenum nitrogenases the active site is the FeMo-cofactor whose structure has been determined in *Azotobacter vinelandii* by X-ray crystallography[5] and comprises a $MoFe_7S_9$ core. The overall structure of FeMo-cofactor is unprecedented, nonetheless the framework of this cluster is composed largely of Fe_2S_2 rhombs. This is one of the basic building blocks for all Fe–S-based clusters including the simple cubane clusters, $[Fe_4S_4(SPh)_4]^{2-/3-}$.

For some time now[6] it has been known that even simple, synthetic Fe–S-based clusters such as $[Fe_4S_4(SPh)_4]^{3-}$ and $[\{MoFe_3S_4(SPh)_3\}(\mu\text{-}SPh)_3]^{4-/5-}$ can reduce H^+ (supplied as a weak acid such as PhSH or $[NHR_3]^+$) to H_2 as shown in eqn. (1).

$$2[Fe_4S_4(SPh)_4]^{3-} + 2PhSH \longrightarrow 2[Fe_4S_4(SPh)_4]^{2-} + 2PhS^- + H_2 \quad (1)$$

These same clusters[7] can also reduce C_2H_2 to C_2H_4 in the presence of an H^+ source. This reaction again mimics the behaviour of the FeMo-cofactor of nitrogenase.[3] In addition, both the natural and synthetic clusters stereospecifically produce *cis*-CHDCHD.

Clearly, establishing the mechanisms of these reactions at synthetic clusters is fundamental to understanding how the metalloenzymes work at the atomic level. Although kinetic studies on H^+ and C_2H_2 reduction by Fe–S-based clusters have been reported[6,8,9] the mechanisms of these transformations are still poorly defined. The main difficulty has been establishing the identity of the solution species. Particularly the protonation state and ligation of the clusters under the conditions in which substrate transformations occur. This paper reports how we have overcome these problems in studying the reduction of H^+ and C_2H_2 by $[Fe_4S_4(SPh)_4]^{3-}$.

Results and discussion

Owing to the complexity of these studies it is important that the mechanistic objectives are clearly set out from the beginning. The work reported, and the order in which it is presented is shown diagrammatically in Fig. 1. Thus, our ultimate goal is to define the mechanism of the conversion of C_2H_2 into C_2H_4 (right hand box). The electrons are supplied from the reduced cluster and H^+ from an acid. It is immediately clear that complications will ensue because, in the presence of acid, the reduced cluster will also reduce H^+ to H_2. Consequently, the mechanism of H_2 production (middle box) must be established before studying the transformation of C_2H_2. In order to understand H^+ reduction we need to define the basic protonation chemistry of these clusters (left hand box). The discussion will follow the approach illustrated in Fig. 1, using $[Hlut]^+$ (lut = 2,6-dimethylpyridine) as the source of H^+ and $[Fe_4S_4(SPh)_4]^{3-}$ as the reduced cluster. The presentation will start with a brief summary of the established protonation chemistry of the oxidised cluster, $[Fe_4S_4(SPh)_4]^{2-}$, then the mechanism for H_2 production from the reduced cluster, $[Fe_4S_4(SPh)_4]^{3-}$, and $[Hlut]^+$ [eqn. (2)] will be discussed, and finally the conversion of C_2H_2 into C_2H_4 [idealised in eqn. (3)] will be described.

$$2[Fe_4S_4(SPh)_4]^{3-} + 2Hlut^+ \longrightarrow 2[Fe_4S_4(SPh)_4]^{2-} + 2lut + H_2 \quad (2)$$

$$2[Fe_4S_4(SPh)_4]^{3-} + 2Hlut^+ + C_2H_2 \longrightarrow 2[Fe_4S_4(SPh)_4]^{2-} + 2lut + C_2H_4 \quad (3)$$

The choice of $[Fe_4S_4(SPh)_4]^{3-}$ was not arbitrary. Initially we, like others before us,[6] screened a variety of structurally well

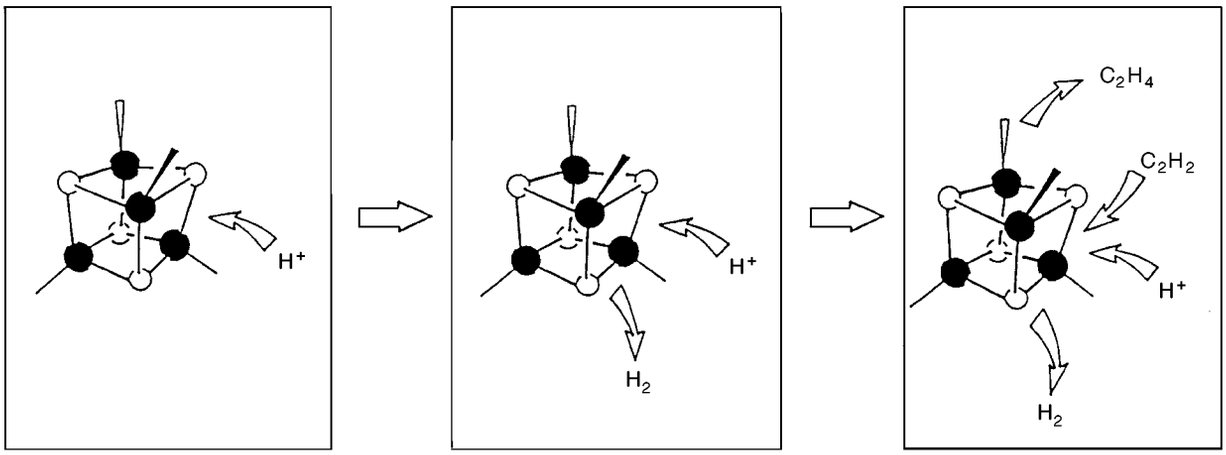

Fig. 1 Schematic representation of the objectives of this study, and the approach taken; Fe = ●, S = ○.

defined synthetic Fe–S-based clusters as candidates for these mechanistic studies;[10–15] $[\{MoFe_3S_4(SPh)_3\}_2(\mu\text{-}SPh)_3]^{5-}$; $[(MoFe_3S_4Cl_3)_2(\mu\text{-}SEt)_3]^{3-}$ with the reductant sodium–acenaphthylene; $[MoFe_3S_4Cl_3(NCMe)(C_6Cl_4O_2)]^{2-}$ with sodium–acenaphthylene; $[Fe_4S_4(SPh)_4]^{3-}$; $[Fe_4S_4(SEt)_4]^{3-}$ and $[Fe_4S_4Cl_4]^{2-}$ with sodium–acenaphthylene. All the systems reduce H^+ to H_2 and C_2H_2 to C_2H_4 but other criteria made $[Fe_4S_4(SPh)_4]^{3-}$ the best cluster to study. Our system (see below) uses mixtures of [Hlut][BPh_4] and [NEt_4][SPh] in MeCN and under these conditions solutions of the chloro-based clusters give black precipitates over the course of a few minutes. Solutions of $[Fe_4S_4(SEt)_4]^{3-}$ or $[\{MoFe_3S_4(SPh)_3\}_2(\mu\text{-}SPh)_3]^{5-}$ remained homogeneous but the kinetics of their reactions was poorly reproducible and so these systems were not pursued.

Using $[Fe_4S_4(SPh)_4]^{3-}$ has three advantages. (i) Both the reactant[13] $[Fe_4S_4(SPh)_4]^{3-}$ and the product[16] $[Fe_4S_4(SPh)_4]^{2-}$ have been structurally characterised. (ii) The conversion of $[Fe_4S_4(SPh)_4]^{3-}$ into $[Fe_4S_4(SPh)_4]^{2-}$ is readily followed by changes in the visible absorption spectra.[17] (iii) The protonation chemistry of $[Fe_4S_4(SPh)_4]^{2-}$ has been defined.[18]

Protonation chemistry of $[Fe_4S_4(SPh)_4]^{2-}$

The kinetics of substitution of Fe–S-based clusters, including $[Fe_4S_4X_4]^{2-}$ (X = thiolate or halide), have been studied.[18,19] In addition, the effect of acid on these kinetics has been investigated [eqn. (4)]. In MeCN the concentrations of EtSH,

$$[Fe_4S_4X_4]^{2-} + EtSH \xrightarrow{[NHR_3]^+} [Fe_4S_4X_3(HSEt)]^- + X^- \quad (4)$$

$[NHR_3]^+$ and NR_3 can be controlled by using mixtures of [NHR_3][BPh_4] and [NEt_4][SEt]. In solution these two species rapidly undergo the protolytic equilibrium (5). This equilibrium

$$[NHR_3]^+ + EtS^- \rightleftharpoons NR_3 + EtSH \quad (5)$$

lies to the right hand side and, provided there is an excess of $[NHR_3]^+$, the amounts of $[NHR_3]^+$, NR_3 and EtSH can be calculated (*i.e.* $[NHR_3^+]_e = [NHR_3^+] - [EtS^-]$ and $[NR_3]_e = [EtSH]_e = [EtS^-]$; from hereon the subscript e designates the calculated concentration present in solution). Thus, by varying the amounts of $[NHR_3]_e$ and EtS^- the concentrations of acid, base and nucleophile can be changed systematically, permitting a detailed kinetic analysis.

These studies showed that $[Fe_4S_4(SPh)_4]^{2-}$ can bind a maximum of three protons and that the state of protonation is defined only by the ratio $[NHR_3^+]_e/[NR_3]_e$ and the strength of the acid. Ethane thiol is a much weaker acid than $[NHR_3]^+$ and at the concentrations used does not contribute to the protonation of the cluster.[20] The successive protonation of the μ_3-S atoms increasingly labilises the cluster towards substitution. By comparison of the results with a variety of Fe–S-based clusters, the sites and sequence of protonations are indicated to be those in Scheme 1.

With either $[NHEt_3]^+$ ($pK_a = 18.46$)[21] or $[Hlut]^+$ ($pK_a = 14.1$)[21] the data are consistent with initial protonation of a thiolate ligand and a second protonation at a μ_3-S atom. Analysis of the kinetics shows that protonation of the μ_3-S is associated with $pK_a = 18.6$.[19] With the stronger acid, $[Hlut]^+$ protonation of a further μ_3-S is observed with $pK_a = 13.7$.[18] It is definition of this protonation chemistry which allows us, for the first time, to establish the protonation state of $[Fe_4S_4(SPh)_4]^{3-}$ which evolves H_2.

Characteristics of H_2 production

Knowing the pK_as associated with protonation of $[Fe_4S_4(SPh)_4]^{2-}$, solutions of $[Fe_4S_4(SPh)_3(SHPh)]^-$, $[Fe_4S_3(SH)(SPh)_3(SHPh)]$ and $[Fe_4S_2(SH)_2(SPh)_3(SHPh)]^+$ can be prepared using mixtures of $[NHR_3]^+$ and PhS^-. To ensure that the ligands on the cluster do not change the system shown in eqn. (6)

$$[NHR_3]^+ + PhS^- \rightleftharpoons NR_3 + PhSH \quad (6)$$

is used. Since PhS^- is also the ligand on the cluster no net substitution can occur.

When $[NHEt_3^+]_e/[NEt_3]_e \geqslant 5.0$ the dominant solution species is $[Fe_4S_3(SH)(SPh)_3(SHPh)]$ and when $[Hlut^+]_e/[lut]_e \geqslant 3.0$ the dominant species is $[Fe_4S_2(SH)_2(SPh)_3(SHPh)]^+$. In the same way the correspondingly protonated forms of $[Fe_4S_4(SPh)_4]^{3-}$ can be prepared, as shown in Scheme 2.

Three solutions were prepared. In all three the total concentration of acid was the same ($[NHR_3^+]_e = 30$ mmol dm^{-3}, $[PhS^-]_e = 6$ mmol dm^{-3}), and present in an excess $\{[NHR_3^+]_e/[Fe_4S_4(SPh)_4^{3-}] = 6\}$. However, in each solution $[NHR_3^+]_e/[NR_3]_e$ was different, resulting in the formation of differently protonated clusters. Analysis of the gas mixtures from each flask shows that only under conditions where $[Fe_4S_2(SH)_2(SPh)_3(SHPh)]$ is formed appreciable amounts of H_2 are produced. The small amounts of H_2 produced from $[Fe_4S_3(SH)(SPh)_3(SHPh)]^-$ were not improved by leaving the mixture for protracted periods (48 h).

The problem inherent in this approach is that although the proton affinities of $[Fe_4S_4(SPh)]_4^{2-}$ are known,[18,19] those of

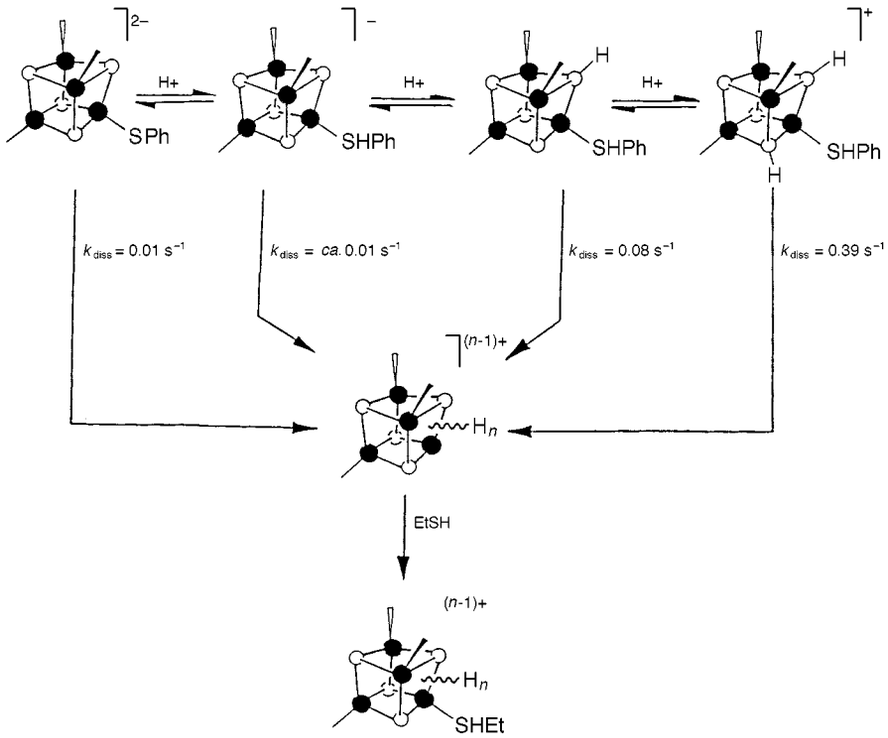

Scheme 1 The effect of protonating $[Fe_4S_4(SPh)_4]^{2-}$ on the rate of dissociation of the lability of the Fe–SPh and Fe–SHPh bonds. For clarity only one Fe–SPh group is shown; Fe = ●, S = ○.

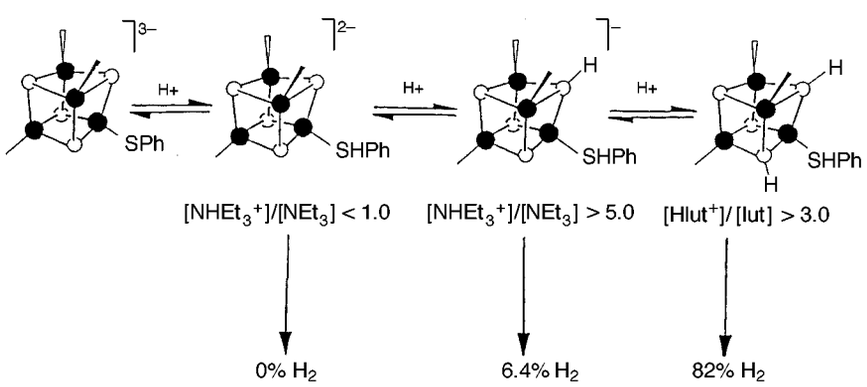

Scheme 2 The effect of protonating $[Fe_4S_4(SPh)_4]^{3-}$ on the ability of the cluster to reduce H^+ to H_2. For clarity only one Fe–SPh group is shown; Fe = ●, S = ○.

$[Fe_4S_4(SPh)_4]^{3-}$ are not. The important point for this study (see below) is that it is reasonable to expect that $[Fe_4S_4(SPh)_4]^{3-}$ is more basic than $[Fe_4S_4(SPh)_4]^{2-}$. Hence, under conditions where we know $[Fe_4S_4(SPh)_4]^{2-}$ is triprotonated ($[Hlut^+]_e/[lut]_e \geqslant 3.$), it is reasonable to assume that $[Fe_4S_4(SPh)_4]^{3-}$ also has three protons bound. In our studies on acid-catalysed substitution reactions[18,19] we have never observed that more than three protons bind to any Fe–S-based cluster.

The yield of H_2 from $[Fe_4S_2(SH)_2(SPh)_3(SHPh)]$ is essentially quantitative provided $[Hlut^+]_e \geqslant 40$ mmol dm^{-3}. At lower concentrations of $[Hlut]^+$ the yield of H_2 is smaller. Similar features have been noted by earlier workers in the reactions of analogous systems.[6] We will return to this problem later.

All the kinetics reported herein were performed in MeCN solutions where $[Hlut^+]_e/[lut]_e \geqslant 5.0$ to ensure that the reduced cluster is present as $[Fe_4S_2(SH)_2(SPh)_3(SHPh)]$. Additionally, the kinetic analysis was simplified by ensuring that (as much as possible) the kinetics was studied under pseudo-first order conditions: $[Hlut^+]_e/[Fe_4S_4(SPh)_4{}^{3-}] \geqslant 10$ and $[PhSH]_e/[Fe_4S_4(SPh)_4{}^{3-}] \geqslant 10$.

The reaction between $[Fe_4S_2(SH)_2(SPh)_3(SHPh)]$ and an excess of $[Hlut]^+$ to produce H_2 occurs in two phases as shown by the typical stopped-flow absorbance *vs.* time curve in Fig. 2. The initial absorbance corresponds to the protonated, reduced cluster $[Fe_4S_2(SH)_2(SPh)_3(SHPh)]$ and the final absorbance to the corresponding oxidised cluster, $[Fe_4S_2(SH)_2(SPh)_3(SHPh)]^+$. There is an initial decrease in absorbance for the first 10 s, followed by an absorbance increase over the next 3 min to produce $[Fe_4S_2(SH)_2(SPh)_3(SHPh)]^+$. The net absorbance change at $\lambda = 600$ nm is that calculated for the quantitative conversion of $[Fe_4S_4(SPh)_4]^{3-}$ ($\varepsilon = 2.9 \times 10^3$ dm^3 mol^{-1} cm^{-1}) into $[Fe_4S_4(SPh)_4]^{2-}$ ($\varepsilon = 4.0 \times 10^3$ dm^3 mol^{-1} cm^{-1}) using absorption coefficients of these two species estimated from the literature.[17] The kinetics of both these phases will be discussed in the following sections, but first we show that H_2 is released in the slow phase.

The slow phase: release of H_2

A typical time course of H_2 release in this system is shown in Fig. 2, superimposed on the absorbance *vs.* time curve. It is clear that H_2 is released in the slow phase. Kinetic analysis shows that the H_2 is produced at a rate which exhibits a first order dependence on the concentration of cluster, but is

Table 1 Kinetic data for the reaction of $[Fe_4S_4(SPh)_4]^{3-}$ with $[Hlut]^+$ in the presence of PhSH, in MeCN at 25.0 °C

$[Hlut^+]_e/[lut]_e$	$[Hlut^+]_e$ [a]/ mmol dm^{-3}	$[PhSH]_e$ [a]/ mmol dm^{-3}	$[C_2H_2]$/ mmol dm^{-3}	k_{obs}/s^{-1}		
				b	*c*	$(k_{obs})^G/s^{-1}$
5.0	1.0	0.2		1.50 (1.60)	0.025 (0.022)	
	2.0	0.4		1.00 (1.10)	0.023 (0.023)	
	2.5	0.5		0.70 (0.65)	0.020 (0.025)	
	5.0	1.0		0.43 (0.35)	0.025 (0.020)	
	10.0	2.0		0.25 (0.28)	0.020 (0.020)	0.018 [d]
	20.0	4.0		0.25 (0.30)	0.022 (0.022)	0.020 [d]
	40.0	8.0				0.017 [d]
10.0	2.0	0.2		1.80 (1.70)	0.025 (0.025)	
	2.5	0.25		1.25 (1.33)	0.028 (0.020)	
	5.0	0.5		0.93 (1.00)	0.025 (0.025)	
	10.0	1.0		0.55 (0.65)	0.023 (0.023)	
	20.0	2.0		0.48 (0.45)	0.020 (0.018)	0.025
20.0	2.0	0.1		1.92	0.020	
	2.5	0.125		1.55	0.023	
	5.0	0.25		1.25	0.028	
	10.0	0.5		1.00	0.020	
	20.0	1.0		0.82	0.025	0.020
5.0	10.0	2.0	20.0			0.018 [e]
	20.0	4.0	20.0			0.015 [e]
	40.0	8.0	20.0			0.020 [e]
	40.0	8.0	10.0			0.016 [e]
5.0	2.0	0.4	*f*	1.10	0.020	
	5.0	1.0		0.40	0.025	
	10.0	2.0		0.25	0.020	
	20.0	4.0		0.25	0.023	

[a] Concentrations presented here are those calculated using eqn. (5) and the relationships presented in the text. [b] Rate constants measured on the stopped-flow apparatus for the fast phase. Values in parentheses are those measured in the presence of $[Dlut]^+$. In general, $[Fe_4S_4(SPh)_4^{3-}] = 2 \times 10^{-5}$ mol dm^{-3}, but see text for full range covered. [c] Rate constants measured on the stopped-flow apparatus for the slow phase. Values in parentheses are those measured in the presence of $[Dlut]^+$. [d] Rate constants for the evolution of H_2, measured using GC; $[Fe_4S_4(SPh)_4^{3-}] = 2 \times 10^{-3}$ mol dm^{-3}. [e] Rate constants for the evolution of C_2H_4, measured using GC; $[Fe_4S_4(SPh)_4^{3-}] = 2 \times 10^{-3}$ mol dm^{-3}. [f] Acetylene was bubbled through the solutions of cluster and $[Hlut]^+/PhS^-$ for *ca.* 10 min immediately prior to the stopped-flow experiments.

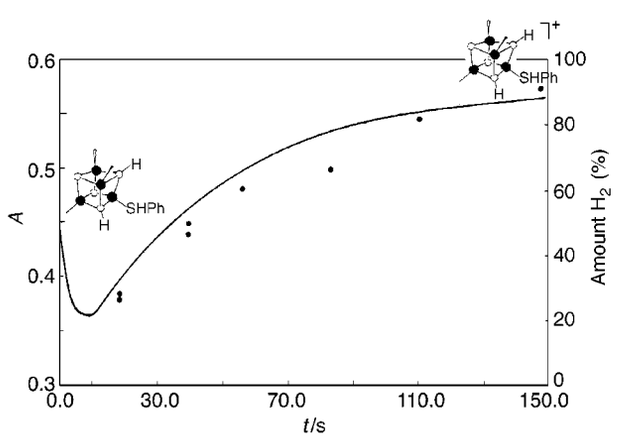

Fig. 2 Typical stopped-flow absorbance *vs.* time curve observed in the H_2-forming reaction between $[Fe_4S_4(SPh)_4]^{3-}$ (1×10^{-4} mol dm^{-3}) and $[Hlut]^+$ ($[Hlut^+]_e = 10$ mmol dm^{-3}) in the presence of PhSH ($[PhSH]_e = 1$ mmol dm^{-3}) in MeCN at 25.0 °C; $[Hlut^+]_e/[lut]_e = 10$. Scale shown on the left hand side. The release of H_2 under the same conditions as measured by GC is also shown (●); scale on the right hand side.

independent of the concentration of $[Hlut]^+$ or PhSH [$k_{obs} = (2.5 \pm 0.3) \times 10^{-2}$ s^{-1}, Table 1]. Kinetic analysis of the absorbance *vs.* time data for the slow phase shows identical kinetics and the same rate constant. This simple observation has important mechanistic consequences.

The stoichiometry of the H_2-forming reaction between $[Fe_4S_4(SPh)_4]^{3-}$ and $[Hlut]^+$ [eqn. (2)] dictates that overall $-d[Fe_4S_4(SPh)_4^{3-}]/dt = 2d[H_2]/dt$. The absorbance *vs.* time curves correspond to changes in the concentration of the cluster, whilst the GC experiments monitor the concentration of H_2. That the same rate constant is observed by monitoring both species dictates that the slow phase must involve a single cluster producing one H_2, and that both electrons required to produce the H_2 must be contained within a single cluster. Consequently, the stoichiometric requirement for two molecules of cluster [eqn. (2)] must have been met in the fast phase of the reaction. We will show later that the H_2-producing cluster is most probably the "super-reduced" $[Fe_4HS_2(SH)_2(SPh)_3]$, but first the kinetics for the fast phase (corresponding to the formation of this cluster) will be presented.

The fast phase: formation of $[Fe_4HS_2(SH)_2(SPh)_3]$

The fast phase must correspond to the reorganisation ("priming") of $[Fe_4S_4(SPh)_4]^{3-}$ in preparation for producing H_2. The initial steps in this "priming" process are the rapid protonation to form $[Fe_4S_2(SH)_2(SPh)_3(SHPh)]$. Earlier studies [18,19] on the acid-catalysed substitution reactions of Fe–S-based clusters showed that these protonations are complete within the dead-time of the stopped-flow apparatus. Thus, the absorbance change and associated kinetics must correspond to other changes to the cluster.

Under all conditions reported herein the fast phase exhibits a first order dependence on the concentration of cluster. This is evident by the good fit of the trace to an exponential curve, and is confirmed by studies in which the concentration of cluster was varied in the range $[Fe_4S_4(SPh)_4^{3-}] = 0.02$–$0.2$ mmol dm^{-3}, with $[Hlut^+]_e = 10$ mmol dm^{-3} and $[PhSH]_e = 1$ mmol dm^{-3}. Under these conditions the observed rate constant did not vary, $k_{obs} = 0.55 \pm 0.05$ s^{-1}.

The dependence on the concentrations of $[Hlut]^+$ and PhSH are complicated as shown by the data in Fig. 3. Each curve

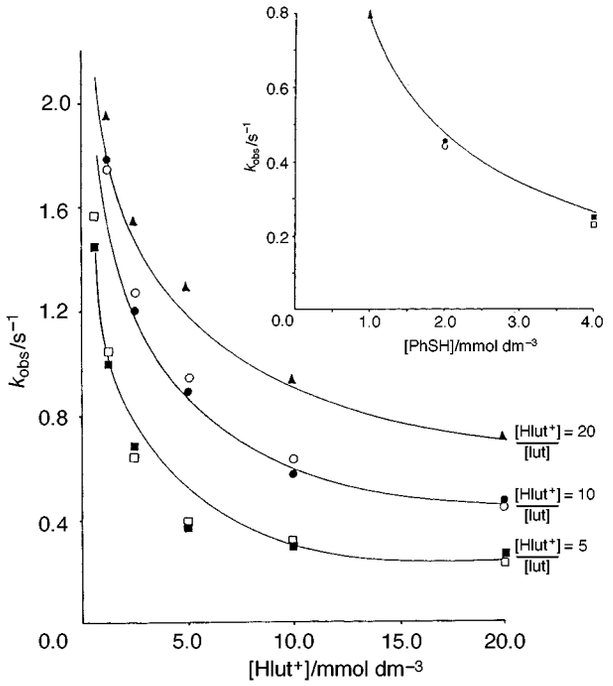

Fig. 3 Main: kinetics for the fast phase in the reaction between $[Fe_4S_4(SPh)_4]^{3-}$ (1×10^{-4} mol dm^{-3}) and $[Hlut]^+$ in the presence of PhSH in MeCN at 25.0 °C. The reaction being followed is the formation of $[Fe_4HS_2(SH)_2(SPh)_3]$. The open symbols correspond to studies using $[Dlut]^+$ (70% labelled). No isotope effects are evident in these reactions. Curves drawn are those defined by eqn. (7). Insert: effect of varying the concentration of PhSH on the kinetics of formation of $[Fe_4HS_2(SH)_2(SPh)_3]$ when $[Hlut^+]_e = 20.0$ mmol dm^{-3}. Curve drawn is that defined by eqn. (7).

corresponds to data where $[Hlut^+]_e/[lut]_e$ is constant, and the concentrations of $[Hlut]^+$ and PhSH are varied. This is a limitation of the approach we have taken. Keeping $[Hlut^+]_e/[lut]_e$ constant whilst varying the concentration of $[Hlut]^+$ necessarily involves varying the concentration of PhSH. Nonetheless, under any condition the concentrations of all the species in solution can be calculated, and hence the kinetics analysed rigorously.

Four features are evident from these data. (i) At low concentrations of $[Hlut]^+$ all data converge to a common rate constant ($k_{obs} = 2.5 \pm 0.5$ s^{-1}). (ii) The rate decreases with increasing concentration of $[Hlut]^+$. (iii) The rate decreases with increasing concentrations of PhSH (Fig. 3, insert). (iv) At high concentrations of $[Hlut]^+$ and PhSH the rate is independent of the concentration of $[Hlut]^+$ but still exhibits an inverse dependence on the concentration of PhSH (Fig. 3, insert).

The rate law for the fast phase [eqn. (7)] was determined by

$$\frac{-d[Fe_4S_2(SH)_2(SPh)_3(SHPh)]}{dt} = \frac{(2.5 + 200[Hlut^+]_e)[Fe_4S_2(SH)_2(SPh)_3(SHPh)]}{1 + 100[Hlut^+]_e + 5200[PhSH]_e} \quad (7)$$

analysing the kinetic data by an iterative procedure. In this approach a series of approximate fits to all the data are refined until the best fit (as shown in Fig. 3) is obtained. Eqn. (7) describes mathematically the "priming" of $[Fe_4S_2(SH)_2(SPh)_3(SHPh)]$, in preparation to form H_2. There are two terms in the numerator of this equation and it is fundamental to any mechanistic interpretation to know if both terms are associated with H_2 production. We can establish this by varying the concentration of $[Hlut]^+$ and measuring the yield of H_2. There are three possible scenarios as shown in Fig. 4.

If both terms in the numerator are associated with H_2 production then H_2 yields will be independent of the concentration of $[Hlut]^+$. However, if only the $[Hlut^+]$-independent term is

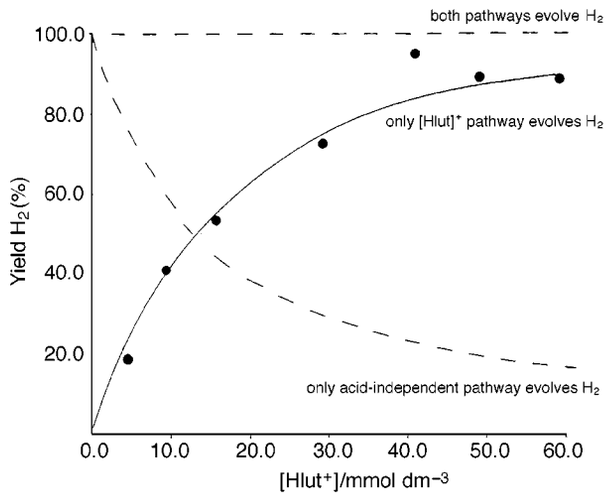

Fig. 4 Effect of the acid concentration on the yield of H_2 in the reaction between $[Fe_4S_4(SPh)_4]^{3-}$ (2×10^{-3} mol dm^{-3}) and $[Hlut]^+$ in the presence of PhSH in MeCN at 25.0 °C: $[Hlut^+]_e/[lut]_e = 5.0$. Curves are those defined by eqn. (7).

associated with H_2 production then H_2 yields will decrease with increasing concentrations of acid. Finally, if only the $[Hlut^+]$-dependent pathway is associated with H_2 production then H_2 yields will increase with increasing concentrations of acid. The data in Fig. 4 show that the yield of H_2 increases with the concentration of $[Hlut]^+$, and the behaviour is quantitatively that predicted by eqn. (7) as shown by the solid curve. Although the yield of H_2 varies, quantitative oxidation of the cluster occurs at all concentrations of $[Hlut]^+$. Clearly, at low concentrations of $[Hlut]^+$ the cluster must be reducing something other than H^+. We will address this problem in the next section.

Mechanism of H_2 formation

We are now in a position to discuss the mechanism of H_2 production in the reaction of $[Hlut]^+$ with $[Fe_4S_4(SPh)_4]^{3-}$, Scheme 3. Initially, we will restrict our attention to the pathway resulting in the quantitative formation of H_2 and oxidised cluster. This is the exclusive pathway operating when $[Hlut^+] \geqslant 40$ mmol dm^{-3}.

Consider first the fast phase. Initial triprotonation of $[Fe_4S_4(SPh)_4]^{3-}$ forms $[Fe_4S_2(SH)_2(SPh)_3(SHPh)]$ within 2 ms, and labilises the cluster to dissociation (k_1 step) to give $[Fe_4S_2(SH)_2(SPh)_3]$. This labilisation is consistent with earlier studies[18] on the acid-catalysed substitution reactions of $[Fe_4S_4(SPh)_4]^{2-}$. It is this dissociation which gives rise to the [PhSH] term in the denominator of eqn. (7). Subsequently, protonation of $[Fe_4S_2(SH)_2(SPh)_3]$ by $[Hlut]^+$ (probably at the Fe from which the thiol dissociated), gives $[Fe_4HS_2(SH)_2(SPh)_3]^+$.

The next step in the mechanism is the reduction of $[Fe_4HS_2(SH)_2(SPh)_3]^+$ {probably by $[Fe_4S_2(SH)_2(SPh)_3(SHPh)]$}, which produces $[Fe_4HS_2(SH)_2(SPh)_3]$ {and one molecule of oxidised cluster, $[Fe_4S_2(SH)_2(SPh)_3(SHPh)]^+$}. It is this 50:50 mixture of oxidised and "super-reduced" clusters which are produced at the end of the fast phase.

Although the kinetics of neither the fast nor the slow phase gives direct information about the electron-transfer step between $[Fe_4S_2(SH)_2(SPh)_3(SHPh)]$ and $[Fe_4HS_2(SH)_2(SPh)_3]^+$, this reaction must occur at this stage in the mechanism for two reasons. First, the kinetics of the fast phase exhibits a strict first order dependence on the concentration of cluster. Secondly, the kinetics for the slow phase shows that one molecule of cluster produces one molecule of H_2. Hence electron transfer must occur *after* the rate-limiting step of the fast phase and *before* the slow phase.

Electron-transfer rates between Fe–S clusters are rapid. For example, the rate of electron self-exchange for $[Fe_4S_4(SC_6$-

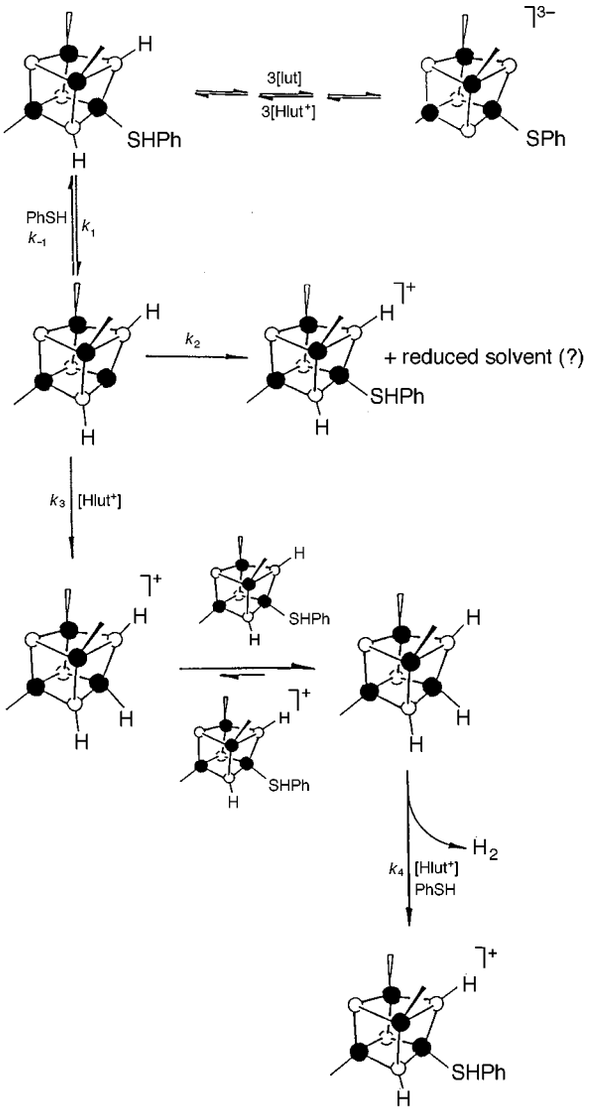

Scheme 3 Proposed mechanism for the reduction of H^+ to H_2 in the reaction between $[Fe_4S_4(SPh)_4]^{3-}$ and $[Hlut]^+$ in MeCN. For clarity only one Fe–SPh group is shown; Fe = ●, S = ○.

$H_4Me)_4]^{2-/3-}$ is $k = 2.8 \times 10^6$ dm^3 mol^{-1} s^{-1} (28 °C).[22] It seems likely that the electron-transfer step in the mechanism of Scheme 3 would be facilitated between two reduced clusters of different charge such as $[Fe_4HS_2(SH)_2(SPh)_3]^+$ and $[Fe_4S_2(SH)_2(SPh)_3(SHPh)]$. That a protonated cluster is reducible by its conjugate base has been proposed earlier.[6]

The rate law for the fast phase is given in eqn. (8). This

$$\frac{-\mathrm{d}[Fe_4S_2(SH)_2(SPh)_3(SHPh)^{3-}]}{\mathrm{d}t} = \frac{k_1(k_2 + k_3[Hlut^+])[Fe_4S_2(SH)_2(SPh)_3(SHPh)^{3-}]}{k_2 + k_3[Hlut^+] + k_{-1}[PhSH]} \quad (8)$$

equation is derived using the steady-state approximation assuming that: (i) initial triprotonation of $[Fe_4S_4(SPh)_4]^{3-}$ occurs within the dead-time of the stopped-flow apparatus; (ii) the dissociation of PhSH (k_1 step), or the protonation (k_3 step), is rate-limiting and, (iii) the electron-transfer step occurs rapidly at the end of the fast phase.

Eqn. (8) includes the k_2 term which describes the non-H_2-producing route which is evident at low concentrations of $[Hlut]^+$ (see below). Comparison of eqns. (7) and (8) gives $k_1 = 2.5 \pm 0.3$ s^{-1}, $k_3/k_2 = 100 \pm 10$ dm^3 mol^{-1} s^{-1} and $k_{-1}/k_2 = (5.2 \pm 0.8) \times 10^3$ dm^3 mol^{-1}.

The kinetics of H_2 production from $[Fe_4HS_2(SH)_2(SPh)_3]$ is

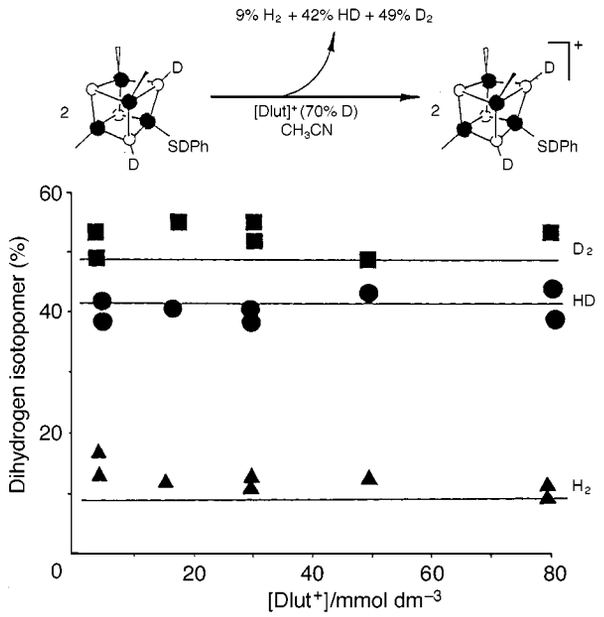

Fig. 5 Yields of H_2, HD and D_2 in the reaction between $[Fe_4S_4(SPh)_4]^{3-}$ (2×10^{-3} mol dm^{-3}) and $[Dlut]^+$ (70% labelled) in MeCN at 25.0 °C. In these experiments no $[NEt_4][SPh]$ was added. Note that the relative proportions do not vary with the concentration of $[Dlut]^+$. The lines drawn are the product distributions predicted assuming that both atoms in the dihydrogen isotopomer are derived from the D-labelled acid as shown in the equation at the top of this Figure.

determined from the data for the slow phase. The rate law is very simple and is shown in eqn. (9), with $k_4 = (2.5 \pm 0.4) \times$

$$\frac{\mathrm{d}[H_2]}{\mathrm{d}t} = \frac{-\mathrm{d}[Fe_4HS_2(SH)_2(SPh)_3]}{\mathrm{d}t} = k_4[Fe_4HS_2(SH)_2(SPh)_3]^+ \quad (9)$$

10^{-2} s^{-1}. Indeed, these kinetics are so simple that they give no information about how the cluster facilitates the coupling of two hydrogen atoms. If the probable structure of $[Fe_4HS_2(SH)_2(SPh)_3]$ (Scheme 3) is considered, it is clear that the hydrogen atoms on two μ_3-SH, or a μ_3-SH and an Fe–H, are too far apart to couple. However, if any of the H atoms can migrate around the cluster core this could facilitate H_2 formation.

We have shown that both hydrogen atoms of H_2 are derived from the acid using isotopically labelled $[Dlut]^+$ (70 ± 10% labelled). Mass spectrometric analysis of the product mixture of H_2, HD and D_2 (Fig. 5) is in good agreement with that calculated assuming coupling of two hydrogens both of which are 70% D-labelled.

Inspection of the whole mechanism shows, rather unexpectedly, that it is necessary to dissociate a thiol ligand before H_2 production is possible. There are two possible reasons for this. (i) Since the co-ordinated thiol is a good electron-withdrawing group its dissociation effectively increases the electron density at the iron site and facilitates protonation. (ii) Dissociation of the thiol may be necessary for the sterically demanding $[Hlut]^+$ to get sufficiently close to protonate the Fe.

We noted earlier that at low concentrations of $[Hlut]^+$ quantitative oxidation of the cluster is associated with less than quantitative amounts of H_2 (Fig. 4). In order to account for this we propose that the cluster must relatively slowly reduce another component of the reaction mixture; most probably either the solvent or possibly phenyl groups of PhSH or $[BPh_4]^-$. This (the k_2 step) is the dominant pathway at low concentrations of $[Hlut]^+$. At higher concentrations of acid, $[Fe_4S_2(SH)_2(SPh)_3]$ is efficiently "captured" by protonation to form $[Fe_4HS_2(SH)_2(SPh)_3]^+$ and this commits the system to producing H_2. We have been unable to detect unambiguously the reduced products at low concentrations of $[Hlut]^+$ using GC or NMR spectroscopy. A major problem is that the system con-

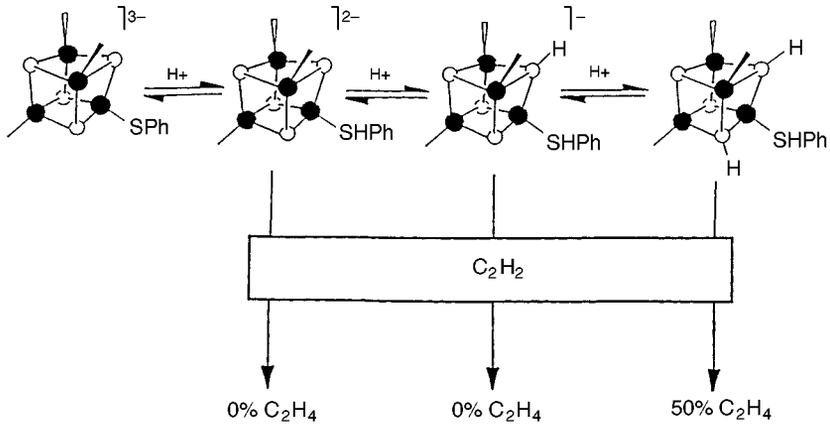

Scheme 4 The effect of protonating $[Fe_4S_4(SPh)_4]^{3-}$ on the ability of the cluster to reduce C_2H_2 to C_2H_4. For clarity only one Fe–SPh group is shown; Fe = ●, S = ○.

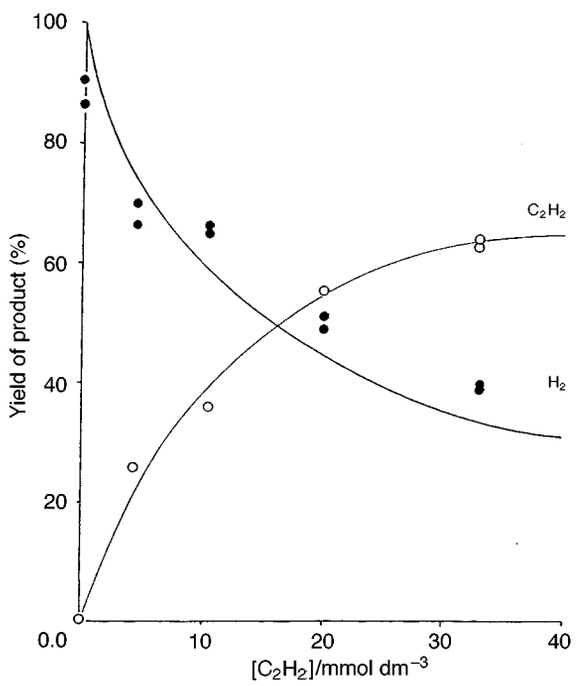

Fig. 6 Effect of varying the concentration of C_2H_2 on the yields of C_2H_4 and H_2 in the reaction between $[Fe_4S_4(SPh)_4]^{3-}$ (2×10^{-3} mol dm^{-3}) and $[Hlut]^+$ (50 mmol dm^{-3}) in the presence of PhSH (10 mmol dm^{-3}) in MeCN at 25.0 °C: $[Hlut^+]/[lut] = 5.0$. Curves are those defined by eqns. (12) and (13).

tains a variety of components essential to control the protonation state of the cluster species in solution and the small amounts of reduced products in this mixture are difficult to detect.

Mechanism of C_2H_4 formation

Introduction of C_2H_2 into this system, containing $[Fe_4S_4(SPh)_4]^{3-}$, $[Hlut]^+$ and PhS^-, results in the formation of C_2H_4. Moreover, C_2H_2 is converted into C_2H_4 only under conditions where $[Fe_4S_2(SH)_2(SPh)_3(SHPh)]$ is the dominant solution species (*i.e.* the same species which reduces H^+ also reduces C_2H_2; Scheme 4).

Following the approach shown in Scheme 2, the protonation state of $[Fe_4S_4(SPh)_4]^{3-}$ in solution was controlled by varying $[NHEt_3^+]_e/[NEt_3]_e$ or $[Hlut^+]_e/[lut]_e$. Only under conditions where $[Fe_4S_2(SH)_2(SPh)_3(SHPh)]$ is formed ($[Hlut^+]_e/[lut]_e \geqslant 3.0$) C_2H_4 is produced. The complex $[Fe_4S_2(SH)_2(SPh)_3(SHPh)]$ also produces quantitative amounts of H_2 when $[Hlut^+]_e \geqslant 40$ mmol dm^{-3}. It is these conditions which were employed to study C_2H_2 reduction. Under them the amount of C_2H_2 was varied and the yields of C_2H_4 and H_2 were determined. The distribution of gaseous products is shown in Fig. 6. In the absence of C_2H_2 (left hand side) quantitative yields of H_2 are produced. The introduction of C_2H_2 decreases the yield of H_2 at the expense of C_2H_4 being produced.

There are three important features about these data. (i) As the concentration of C_2H_2 is increased the yield of C_2H_4 increases and the yield of H_2 decreases proportionately. At all concentrations of C_2H_2 the combined yields of C_2H_4 and H_2 account for 98 ± 10% of the available electrons from the reduced cluster. (ii) The identity of C_2H_4 was established unambiguously using GC–mass spectrometry. Some C_2H_6 was also detected but this never accounted for more than *ca.* 5% of the total yield. This has been observed before in other systems,[8] (iii) When $[C_2H_2] \geqslant 25$ mmol dm^{-3} the product distribution is constant (30% H_2 and 70% C_2H_4), with the resulting stoichiometry at high concentrations of C_2H_2 described by eqn. (10).

$$2[Fe_4S_4(SPh)_4]^{3-} + 2[Hlut^+] + 0.7C_2H_2 \longrightarrow 2[Fe_4S_4(SPh)_4]^{2-} + 0.7C_2H_4 + 0.3H_2 + 2lut \quad (10)$$

This behaviour indicates that each cluster has a C_2H_2 bound when $[C_2H_2] \geqslant 25$ mmol dm^{-3}, but that this species still produces H_2 30% of the time. Quantitative analysis of the product distribution data gives the apparent equilibrium constant for C_2H_2 binding to $[Fe_4S_2(SH)_2(SPh)_3(SHPh)]$, as defined by eqn. (11). This is an *apparent* equilibrium constant since, as we shall

$$[Fe_4S_2(SH)_2(SPh)_3(SHPh)] + C_2H_2 \overset{K_0}{\rightleftharpoons} [Fe_4S_2(SH)_2(SPh)_3(SHPh)(C_2H_2)] \quad (11)$$

see, the cluster species which binds C_2H_2 is probably $[Fe_4HS_2(SH)_2(SPh)_3]^+$. It is easy to show that, when half of the cluster has C_2H_2 co-ordinated, $[Fe_4S_2(SH)_2(SPh)_3(SHPh)]_e = [Fe_4S_2(SH)_2(SPh)_3(SHPh)(C_2H_2)]_e$ and $K_0 = 1/[C_2H_2]$. Analysis of the data in Fig. 6 gives $K_0 = 143 \pm 20$ dm^3 mol^{-1}.

The mechanism consistent with this product distribution is shown in Scheme 5. In this mechanism the initial elementary reactions involving the formation of $[Fe_4HS_2(SH)_2(SPh)_3]^+$ are those seen in the H_2-forming mechanism (Scheme 3). It seems most likely that C_2H_2 binds at the vacant site on the Fe from which the thiol has dissociated. Subsequent electron transfer from another reduced cluster produces the "super-reduced" cluster, $[Fe_4HS_2(SH)_2(SPh)_3(C_2H_2)]$. The intimate mechanism of the conversion of bound C_2H_2 into C_2H_4 cannot be defined from the available data but could occur either by intramolecular hydrogen atom transfer from hydrogens bound to the cluster or by protonation from $[Hlut]^+$.

Apart from containing a C_2H_2 ligand, $[Fe_4HS_2(SH)_2(SPh)_3$-

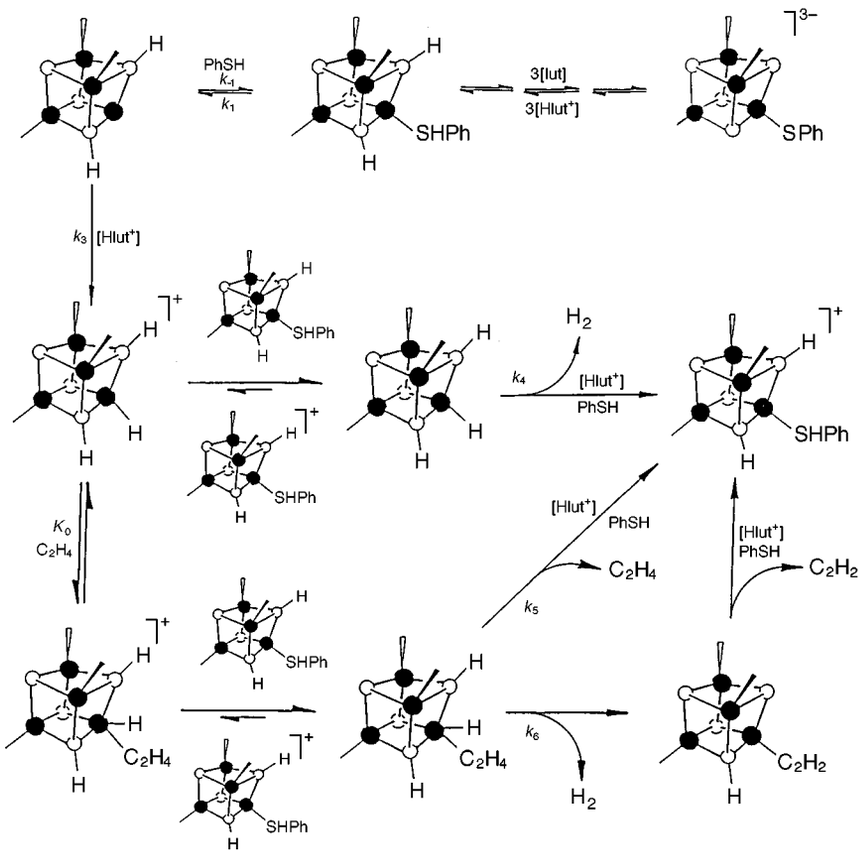

Scheme 5 Proposed mechanism for the reduction of C_2H_2 to C_2H_4 in the reaction between $[Fe_4S_4(SPh)_4]^{3-}$ and $[Hlut]^+$ in MeCN. Also shown are the H_2-forming pathways, both in the absence and presence of C_2H_2. For clarity only one Fe–SPh group is shown; Fe = ●, S = ○.

$(C_2H_2)]$ is identical to $[Fe_4HS_2(SH)_2(SPh)_3]$ the species which produces H_2 (Scheme 3). It is not surprising therefore that it can still produce H_2 30% of the time. Simplistically, co-ordinated C_2H_2 is an insufficiently good "electron sink" to ensure that electrons are routed only into formation of C_2H_4. The alternative pathway involving release of H_2 from $[Fe_4HS_2(SH)_2(SPh)_3(C_2H_2)]$ results in the formation of the oxidised cluster and dissociation of C_2H_2.

Analysis of the product distribution allows us to calculate the values of k_5 and k_6. The yields of C_2H_4 and H_2 are related to the elementary rate and equilibrium constants as described by eqns. (12) and (13) respectively (see Appendix). The value $K_0 = 143 \pm$

$$\text{Proportion of } C_2H_4 = \frac{k_5K_0[C_2H_2]}{k_4 + K_0(k_5 + k_6)[C_2H_2]} \quad (12)$$

$$\text{Proportion of } H_2 = \frac{k_4 + k_6K_0[C_2H_2]}{k_4 + K_0(k_5 + k_6)[C_2H_2]} \quad (13)$$

20 dm^3 mol^{-1} was estimated above, and the kinetics of the H_2-forming reaction gave $k_4 = (2.5 \pm 0.4) \times 10^{-2}$ s^{-1}. Using these values, eqns. (12) and (13) can be solved giving $k_5 = (1.3 \pm 0.3) \times 10^{-2}$ s^{-1} and $k_6 = (0.9 \pm 0.1) \times 10^{-2}$ s^{-1}.

The value $k_5 = (1.7 \pm 0.3) \times 10^{-2}$ s^{-1} has been determined experimentally by monitoring the release of C_2H_4 by GC (Table 1). However, the apparently good agreement of this value with the value of k_5 determined using eqns. (12) and (13) should be treated with some caution. In the kinetic experiments the amount of C_2H_2 introduced into the flask would correspond to a concentration in solution of 10 or 20 mmol dm^{-3}, if it all dissolved. It seems unlikely that the concentration of C_2H_2 in solution is as high as 10–20 mmol dm^{-3} but rather the C_2H_2 is partitioned between the gaseous and liquid phases. How this affects the kinetic analysis is not clear. If the diffusion of C_2H_2 across the interface is faster than the rate of C_2H_4 release then effectively the concentration of C_2H_2 in solution is 20 mmol dm^{-3}. However, if the diffusion is slow the concentration of C_2H_2 in solution is more likely to be 1–2 mmol dm^{-3}.

The similarity in the values of k_4, k_5 and k_6 is consistent with the results of stopped-flow studies on the reaction between $[Fe_4S_4(SPh)_4]^{3-}$ and $[Hlut]^+$ in a saturated solution of C_2H_2. The absorbance *vs.* time curves are identical to those observed when only H_2 is being produced (*i.e.* in the absence of C_2H_2). Analysis of the kinetic data (Table 1) for both phases gave results indistinguishable from those where only H_2 is being produced.

Comparisons with other studies: H_2 production

The mechanisms in Schemes 3 and 5 present a unified picture for the mechanisms of H^+ and C_2H_2 reduction by $[Fe_4S_4(SPh)_4]^{3-}$. These mechanisms are consistent with observations made by earlier workers on the reduction of H^+ and C_2H_2 by structurally analogous Fe–S-based clusters.[6–9] In this last part of the paper we will discuss these earlier results in the context of our mechanism.

Intriguingly, earlier studies[6] on the reaction between $[Fe_4S_4(SPh)_4]^{3-}$ and PhSH [eqn. (1)] in dimethylacetamide showed that a 500-fold excess of PhSH produces only *ca.* 40% yields of H_2, but quantitative oxidation of the cluster to $[Fe_4S_4(SPh)_4]^{2-}$. The reasons why such a large excess of PhSH is necessary has, so far, been unclear. However, the mechanism in Scheme 3 rationalises this behaviour and indicates that the origin of this behaviour is because PhSH is a weak acid in aprotic solvents. This will affect the elementary reactions in the mechanisms in two ways. First, a very large excess of PhSH is necessary to protonate $[Fe_4S_4(SPh)_4]^{3-}$ to $[Fe_4S_2(SH)_2(SPh)_3(SHPh)]$, the protonation state of the cluster which is necessary to produce H_2. Secondly, later in the mechanism, protonation of $[Fe_4S_2(SH)_2(SPh)_3]$ to $[Fe_4HS_2(SH)_2(SPh)_3]^+$ has to occur. If this protonation is slow (*i.e.* low concentrations of the weak acid

$$\frac{d[H_2]}{dt} = \frac{a[PhSH]^2[\{MoFe_3S_4(SPh)_3\}_2(\mu\text{-}SPh)_3^{4-}]^2}{([\{MoFe_3S_4(SPh)_3\}_2(\mu\text{-}SPh)_3^{3-}] + b[PhSH])[PhS^-] + c[PhSH][\{MoFe_3S_4(SPh)_3\}_2(\mu\text{-}SPh)_3^{4-}]} \quad (14)$$

$$\frac{d[H_2]}{dt} = \frac{k_1k_3k_4k_5K_aK_a'[Fe_4S_4(SPh)_3(SHPh)^{2-}]^2[PhSH]^2/[PhS^-]^2}{k_{-1}k_3k_{-5}\{[Fe_4S_4(SPh)_3(SHPh)^-] + (k_4/k_{-5})\}[PhS^-] + k_4k_5(k_{-1} + k_3)[Fe_4S_4(SPh)_3(SHPh)^{2-}]} \quad (15)$$

PhSH), oxidation of the cluster will occur by the non-H_2-producing pathway (k_2 step).

The kinetics of H_2 formation[6] in the reaction between PhSH and the one electron reductant $[\{MoFe_3S_4(SPh)_3\}_2(\mu\text{-}SPh)_3]^{4-}$ has been studied, and analysis of the data gave the empirical rate law (14). Although this is very different to eqns. (8) and (9), it is consistent with the mechanism shown in Scheme 3. The reason the rate laws differ is merely a consequence of using the weak acid PhSH as the proton source, rather than the stronger $[Hlut^+]$. It is the strength of the acid which defines the position of all the protolytic equilibria.

If we consider the behaviour we would expect from $[Fe_4S_4(SPh)_4]^{3-}$ under these conditions, it seems likely that PhSH is only capable of singly protonating this cluster to form $[Fe_4S_4(SPh)_3(SHPh)]^{2-}$, and that with this acid only very small concentrations of $[Fe_4S_3(SH)(SPh)_3(SHPh)]^-$ and $[Fe_4S_2(SH)_2(SPh)_3(SHPh)]$ would be present. Consequently the rate law must take into account the equilibrium constants for protonation of the μ_3-S sites on the cluster. In addition, in the studies with PhSH, the rate of the k_{-3} step must be considered. Since PhSH is a weaker acid than $[Hlut]^+$ it follows that PhS^- is a stronger conjugate base than lut. Thus, if the value of k_{-3} depends on the strength of the base, this reaction will be faster with PhS^- than with lut. Taking into account these changes, it is relatively easy to show (using the steady state approximation) that the mechanism in Scheme 3 is associated with the rate law (15), where K_a and K_a' are the equilibrium constants for protonation of $[Fe_4S_4(SPh)_3(SHPh)]^{2-}$ and $[Fe_4S_3(SH)(SPh)_3(SHPh)]^-$ respectively. This rate law is very similar, but not identical, to eqn. (14). However, without quantitative information concerning the acid strength of PhSH in the solvents used, it is impossible to calculate the relative concentrations of PhSH and PhS^- necessary to fit the experimental data to eqns. (14) and (15) and hence see if these expressions are numerically distinguishable.

Comparisons with other studies: C_2H_4 production

There have been several studies on the reduction of C_2H_2 by a variety of structurally similar Fe–S-based clusters[7–9] including catalytic systems.

The study of C_2H_2 reduction by $[Fe_4S_4(SPh)_4]^{3-}$ in *N*-methylpyrrolidinone used acetic acid as the proton source[6] and observed quantitative yields of oxidised cluster, but a maximum yield of C_2H_4 of *ca.* 60%. No other product was detected. Similarly, in our system, we observe quantitative oxidation of the cluster and a maximum yield of C_2H_4 of *ca.* 70%. However, in addition, a 30% yield of H_2 is obtained giving an electron balance in our system and demonstrating that C_2H_2 cannot entirely suppress the formation of H_2.

In studies on the catalytic formation of C_2H_4 from $[MoFe_3S_4Cl_3(NCMe)(C_6Cl_4O_2)]^{2-}$ and C_2H_2 in the presence of $[Hlut]^+$, using $[Co(\eta^5\text{-}C_5H_5)_2]$ as the reductant, the kinetics of the catalysis has been determined.[8,9] The key kinetic results are consistent with our mechanism in Scheme 5. Thus, the rate of catalysis exhibits a first order dependence on the concentrations of cluster and $[Hlut]^+$ (provided $30 < [Hlut^+] < 100$ mmol dm^{-3}), and a non-linear dependence on the concentration of C_2H_2. Analysis of the C_2H_2 data gives an apparent binding constant of C_2H_2 to $[MoFe_3S_4Cl_3(NCMe)(C_6Cl_4O_2)]^{2-}$ of $K_0 = ca.$ 56 $dm^3\ mol^{-1}$. This value is similar to that determined in this study for $[Fe_4S_4(SPh)_4]^{3-}$.

Finally, an essential feature of our mechanism for C_2H_2 reduction is that PhSH must dissociate from the cluster before C_2H_2 can bind. This is consistent with the results of earlier Raman spectroscopic studies[23] which indicated that only $[Fe_4S_4(SPh)_4]^{3-}$ will bind C_2H_2 but only after dissociation of thiol.

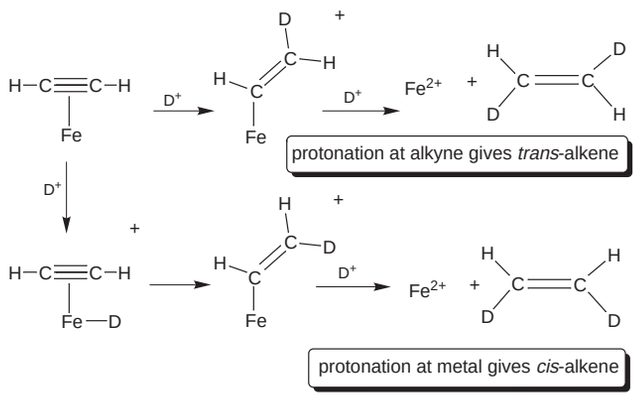

Scheme 6 Pathways for the stereoselective formation of *cis*- or *trans*-CHDCHD from the reaction of C_2H_2 with D^+ at a single Fe.

Stereoselective formation of *cis*-CHDCHD

Although we have not determined the stereochemistry of the C_2H_4 product in our system, it is pertinent to discuss this aspect of the reaction. Earlier studies[7] showed that the reduction of C_2H_2 by $[Fe_4S_4(SPh)_4]^{3-}$ with CD_3CO_2D gives *cis*-CHDCHD. This stereoselectivity is consistent with the mechanism shown in Scheme 5, and earlier studies on stereoselectivity of protonation reactions at simple mononuclear alkyne complexes.[24,25]

The protonation of structurally well defined mononuclear alkyne complexes can result in a *cis*- or *trans*-alkene product depending on the initial site of proton attack, as shown in Scheme 6. Thus, direct protonation of the co-ordinated C_2H_2 gives the *trans*-vinyl species. In contrast, if initial protonation is at the metal, subsequent intramolecular migration of the hydride ligand gives the *cis*-vinyl species. Provided the carbon–carbon double bond is retained throughout the reaction, further protonation will give the corresponding alkene (*i.e.* *cis*-vinyl gives *cis*-alkene and *trans*-vinyl gives *trans*-alkene). The mechanism proposed in Scheme 5 could accommodate either of these two pathways. The observed *cis* stereoselectivity[7] in the reactions involving $[Fe_4S_4(SPh)_4]^{3-}$ is consistent with the most facile pathway being migration of the hydride ligand to C_2H_2 in $[Fe_4HS_2(SH)_2(SPh)_3(C_2H_2)]$.

Conclusion

In this paper we have presented a unified mechanism for the reduction of H^+ to H_2 and C_2H_2 to C_2H_4 by the simple cubane cluster $[Fe_4S_4(SPh)_4]^{3-}$. This mechanism is consistent with all of the kinetic and product analyses presented, and observations made by other workers on these transformations at analogous Fe–S-based clusters.

This study has concentrated on the nature and identity of the cluster species in solution which perform these transformations. What the study does not, and cannot, address are the details of these transformations (*e.g.* the intimate mechanism of H–H coupling which results in H_2, the mode of binding and activation of C_2H_2, where protons bind to co-ordinated C_2H_2 and the structure of the intermediates). These processes occur too rapidly for us to probe them directly using the approach reported.

The ways in which alkynes are transformed in structurally well defined mononuclear complexes have been studied in great detail.[3,25] It is likely that if the same reactions occur on a single metal of these clusters then the mechanisms established on the mononuclear complexes are good models for the behaviour of clusters. This is the basis for the arguments we presented above to rationalise the stereoselective formation of *cis*-CHDCHD. However, if the substrate binds to the cluster in a manner which is not possible on simple mononuclear or binuclear complexes (*e.g.* binding across an Fe_2S_2 face) then the mechanism of transformation has not been defined. Clearly, it is necessary to establish, structurally, the way in which simple unsaturated hydrocarbons bind to Fe–S-based clusters. Not only will this lead to a better understanding of the reactions reported in this paper but also the behaviour of naturally occurring clusters.

Experimental

All manipulations were performed under an atmosphere of dinitrogen using Schlenk or syringe techniques as appropriate.

Acenaphthylene, PhSH and 2,6-dimethylpyridine from Aldrich were used as received. The following materials were prepared by the literature methods: $[NEt_4]_2[Fe_4S_4(SPh)_4]$,[26] $[NEt_4]_3[Fe_4S_4(SPh)_4]$,[15] $[NHEt_3][BPh_4]$[27] and $[NEt_4][SPh]$;[28] $[Hlut][BPh_4]$ (lut = 2,6-dimethylpyridine) was prepared by a method analogous to that of $[NHEt_3][BPh_4]$. The solvents MeCN and thf were freshly distilled from CaH_2 and sodium–benzophenone respectively, immediately prior to use. Solutions of sodium–acenaphthylene (1 mol dm^{-3}) in thf were prepared on the day of use.

Preparation of [Dlut][BPh$_4$]

To a stirred solution of lut (2.2 g, 20 mmol) in thf (*ca.* 50 cm^3) was added MeOD (1.0 cm^3, 30 mmol; 99% D-labelled) and $SiMe_3Cl$ (3.2 cm^3, 30 mmol). The white precipitate of [Dlut]Cl was removed by filtration, washed with thf and then dried *in vacuo*. This solid was dissolved in MeOD and added dropwise to a solution of $NaBPh_4$ in MeOD. The resulting white crystalline material was removed by filtration, washed with water to remove NaCl, then washed with MeOD, and finally dried in air.

The isotopic purity of the product was determined by ^1H and ^2H NMR spectroscopy. ^1H NMR spectrum of $[Hlut][BPh_4]$ in CD_3CN: δ 2.63 (s, 6 H, Me), 6.84 (t, 4 H, J_{HH} = 7.1, Ph), 7.00 (m, 8 H, Ph), 7.28 (m, 8 H, Ph), 7.53 (t, 2 H, J_{HH} = 6.9, lut), 8.18 (t, 1 H, J_{HH} = 6.9 Hz, lut) and 12.37 (s, broad, disappears on addition of CD_3OD, 1 H, *H*lut). The ^1H NMR spectrum of $[Dlut][BPh_4]$ is identical except that the resonance at δ 12.37 is significantly weaker. Integration of this peak and comparison with the integration of the signal at δ 2.63 (s, 6 H, Me) allowed us to calculate that the deuterium isotopic purity was 75 ± 10%. Confirmation that the low field resonance is due to *H*lut came from measuring the ^2H NMR spectrum of $[Dlut][BPh_4]$, which showed a broad resonance at δ 13.05 which was not present in a sample of $[Hlut][BPh_4]$.

Stopped-flow kinetic studies

The kinetics of the reactions between $[NEt_4]_3[Fe_4S_4(SPh)_4]$ and $[Hlut][BPh_4]$, $[NEt_4][SPh]$ and C_2H_2 was studied in MeCN using a Hi-Tech SF-51 stopped-flow spectrophotometer, modified to handle air-sensitive solutions.[29] Dilute solutions of $[NEt_4]_3[Fe_4S_4(SPh)_4]$ were prepared in an anaerobic glove-box (O_2 < 1 ppm). The solutions were transferred to a sealed all-glass syringe, removed from the glove-box and transferred to the stopped-flow apparatus. Solution of $[Hlut][BPh_4]$ with $[NEt_4][SPh]$ were prepared from freshly prepared stock solutions of the two reagents, and used within 1 h of preparation. All solutions were rigorously degassed immediately prior to being introduced into the stopped-flow apparatus.

Owing to the extreme air-sensitivity of $[Fe_4S_4(SPh)_4]^{3-}$ the stopped-flow apparatus was rinsed initially with dilute solutions of sodium–acenaphthylene in thf to purge O_2 from the Teflon tubing of the mixing system, then degassed MeCN, prior to introducing a solution of the cluster. In addition, cluster solution (*ca.* 1 cm^3) was sacrificed in further rinsing the mixing apparatus of the stopped-flow spectrophotometer. The temperature was maintained at 25.0 °C using a Grant LE8 thermostat tank.

The spectrophotometer was interfaced to a Viglen computer *via* an analogue-to-digital converter and the kinetics was monitored by following the absorbance change at $\lambda = 600$ nm, associated with the conversion of $[Fe_4S_4(SPh)_4]^{3-}$ into $[Fe_4S_4(SPh)_4]^{2-}$. Under all the conditions reported the reaction is characterised by a biphasic absorbance *vs.* time curve, typified by that shown in Fig. 2: an initial decrease in absorbance followed by an increase. The whole trace was a good fit to two exponential curves. The fit was performed using a computer program, and the values of the observed rate constants, k_{obs}, were obtained from this analysis.

The kinetics was identical whether the reactions were studied using isolated $[NEt_4]_3[Fe_4S_4(SPh)_4]$ or by generating this species in solution by preparing a solution of $[NEt_4]_2[Fe_4S_4(SPh)_4]$ (in MeCN) and adding 1.5 mol equivalents of sodium–acenaphthylene (in thf). Details of the kinetic analysis to establish the dependence of the reaction rate on the concentrations of $[Hlut]^+$ and PhSH are given in the Results and Discussion section.

Identification of cluster product

The cluster product formed under all the conditions reported in this paper is $[Fe_4S_4(SPh)_4]^{2-}$ or, more correctly, its protonated form $[Fe_4S_2(SH)_2(SPh)_3(SHPh)]^+$. The identity of the product, and that it was formed quantitatively, was established by visible absorption spectroscopy in the following manner. Initially, the visible spectrum of a solution of $[Fe_4S_4(SPh)_4]^{2-}$ (1×10^{-4} mol dm^{-3}) in MeCN was recorded. Addition of 1.5 mol equivalents of sodium–acenaphthylene resulted in a less intense absorption with a spectrum identical to that of authentic $[Fe_4S_4(SPh)_4]^{3-}$. Addition of a solution of $[Hlut]^+$ (10 mmol dm^{-3}) and PhS^- (2 mmol dm^{-3}) produced a spectrum identical to that of $[Fe_4S_4(SPh)_4]^{2-}$ at all wavelengths (λ = 300–800 nm).

Proton NMR spectroscopy could not be used to confirm the identification of the product since resonances from the other components of the reaction mixture (PhSH, $[Hlut]^+$, lut and $[BPh_4]^-$) mask the resonances of the cluster.

Gas chromatographic analysis

Quantitative gas analysis of H_2 and C_2H_4 was performed on a Philips PU 4400 gas chromatograph equipped with a computing integrator. Separation of H_2 was achieved on an alumina column with argon as the carrier gas using a thermal conductivity detector. Hydrocarbon separation was achieved with an alumina column with dinitrogen as the carrier gas, using a flame ionisation detector. Identification and quantification of C_2H_4 and C_2H_6 was by comparison with the retention times of known amounts of authentic samples of these gases.

In general, preparation of a sample for the analysis of H_2 was as follows. The complex $[NEt_4]_2[Fe_4S_4(SPh)_4]$ (0.06 g, 5×10^{-5} mol) was weighed into a one-necked flask (50 cm^3) equipped with a stirrer. To this was added the required amounts of $[Hlut][BPh_4]$ and $[NEt_4][SPh]$. The flask was sealed with a rubber septum and then evacuated and flushed with dinitrogen *via* a needle connector. Freshly distilled MeCN (10 cm^3) was introduced through the septum and the reaction mixture evacuated and flushed with dinitrogen three times. The flask was disconnected from the dinitrogen manifold and the reductant, sodium–acenaphthylene (2 cm^3, 1.0 mmol) introduced to the sealed flask through the rubber septum. After *ca.* 1–2 h a

sample of the gas phase (0.1 cm^3) was taken. Repeated GC sampling was performed to ensure consistency of the result.

In the studies on the reactions with C_2H_2 the same procedure was adopted except that the required amount of C_2H_2 was introduced prior to the addition of the reductant.

Kinetics of H_2 or C_2H_4 production

The time courses for the release of both these gaseous products was monitored by gas chromatography. The sample was prepared as described in the section above. Upon addition of the reductant ($t = 0.0$ s), the stopclock was started, and samples were taken every 30 s up to 5 min, followed by sampling at 10, 20 and 60 min. The concentrations of H_2 and C_2H_4 were calculated from the gas chromatograms by comparison with a standard sample of the gas. The rate constant associated with the production of these gases was determined from the usual semi-logarithmic plots of $\log_e[H_2]$ (or $\log_e[C_2H_4]$) against time.[30] These plots were good straight lines for at least 2–3 half-lives and the rate constants were determined from the gradient of the line.

Mass spectrometry

For the reaction between $[Fe_4S_4(SPh)_4]^{3-}$ and $[Dlut]^+$ (70% D-labelled), the H_2, HD, D_2 product distribution was determined using a MassTorr DX quadrupole analyser mass spectrometer, operating at a sample pressure of 58.6 mbar (bar = 10^5 Pa). The peak heights of the H_2 isotopomers were corrected for the analyser response using calibration curves established with reference samples of H_2, HD and D_2.

The gas samples from the reaction of $[Fe_4S_4(SPh)_4]^{3-}$ with $[Dlut]^+$ were prepared in the same way as described above. However, for the mass spectrometry studies a 10 cm^3 gaseous sample was taken. Owing to this large volume only three samples were taken: at 30 min; 1 and 2 h. In all three samples the relative amounts of the three H_2 isotopomers was constant.

GC–Mass spectrometry

The GC–mass spectra were recorded at the Instituto Superior Tecnico in Lisbon, Portugal, using a GC–MS Carlo Erba Auto/HRGC/MS instrument with a Fisons quadrupole. The GC carrier gas was helium (2 $cm^3\ min^{-1}$) with a PLOT fused silica Al_2O_3/Na_2SO_4 capillary column. The oven temperature was 50 °C (for 5 min) ramping to 150 °C (over 30 min). The injector and source temperatures were 150 °C.

Samples for GC–MS were prepared in the same way as those for the GC experiments. The sample injection size was 500 μl. The hydrocarbons were identified by their retention times on the GC separation and comparison of the mass spectral cracking pattern with those of authentic samples of C_2H_4 and C_2H_6.

Appendix

Derivation of eqns. (12) and (13)

In deriving these relationships between the yields of H_2 and C_2H_4 and the elementary rate and equilibrium constants in the reactions with $[Fe_4S_4(SPh)_4]^{3-}$ the reader is referred to Scheme 5.

As discussed in the text, the initial phase of the reaction involves the formation of $[Fe_4HS_2(SH)_2(SPh)_3]$. In the absence of C_2H_2, this "super-reduced" cluster evolves H_2 at a rate described by eqn. (A1).

$$d[H_2]/dt = k_4[Fe_4HS_2(SH)_2(SPh)_3] \quad (A1)$$

In the presence of C_2H_2, $[Fe_4HS_2(SH)_2(SPh)_3]$ binds C_2H_2 in an equilibrium reaction (K_0) to produce $[Fe_4HS_2(SH)_2(SPh)_3(C_2H_2)]$. This species can produce H_2 or C_2H_4 by the pathways shown in Scheme 5, and at a rate described by eqns. (A2) and (A3) respectively. The subscript e in eqns. (A1), (A2) and (A3)

$$d[H_2]/dt = k_6K_0[Fe_4HS_2(SH)_2(SPh)_3]_e[C_2H_2] \quad (A2)$$

$$d[C_2H_4]/dt = k_5K_0[Fe_4HS_2(SH)_2(SPh)_3]_e[C_2H_2] \quad (A3)$$

designates the equilibrium concentration of $[Fe_4HS_2(SH)_2(SPh)_3]$ formed in solutions containing C_2H_2. The total rate observed is the summation of these equations, and the yields of C_2H_4 and H_2 are proportional to the rates at which these products are formed. For C_2H_4 this is relatively simple since only one pathway [eqn. (A3)] involves production of this gas. For H_2 both eqns. (A2) and (A1) are necessary to describe the C_2H_2-independent and -dependent formation of H_2.

Thus, the proportion of the total reaction which produces C_2H_4 is given by eqn. (A4). Collecting together like terms and cancelling gives eqn. (12). Similarly, the proportion of the total reaction which produces H_2 is given by eqn. (A5) which can be rearranged into (13).

Acknowledgements

We thank BBSRC for supporting this work. K. L. C. G. thanks the John Innes Foundation for a studentship. We thank Professor Armando J. L. Pombeiro for his hospitality and permission to use the GC–MS facilities in Lisbon, and Mr. Indalécio Marques for running these spectra.

References

1 R. H. Holm, P. Kennepohl and E. I. Solomon, *Chem. Rev.*, 1996, **96**, 2239 and refs. therein.
2 R. Cammack, *Adv. Inorg. Chem.*, 1988, **32**, 297 and refs. therein.
3 D. J. Evans, R. A. Henderson and B. E. Smith, *Bioinorganic Catalysis*, ed. J. Reedijk, Marcel Dekker, New York, 1993, p. 89 and refs. therein.
4 M. W. W. Adams, *Biochim. Biophys. Acta*, 1990, **1020**, 115 and refs. therein.
5 J. Kim, D. Woo and D. C. Rees, *Biochemistry*, 1993, **32**, 7104 and refs. therein.
6 T. Yamamura, G. Christou and R. H. Holm, *Inorg. Chem.*, 1983, **22**, 939.
7 R. S. McMillan, J. Renauld, J. G. Reynolds and R. H. Holm, *J. Inorg. Biochem.*, 1979, **11**, 213.
8 L. J. Laughlin and D. Coucouvanis, *J. Am. Chem. Soc.*, 1995, **117**, 3118.
9 D. Coucouvanis, *J. Bioinorg. Chem.*, 1996, **1**, 594 and refs. therein.
10 G. Christou, P. K. Mascharak, W. H. Armstrong, G. C. Papaefthymiou, R. B. Frankel and R. H. Holm, *J. Am. Chem. Soc.*, 1982, **104**, 2820.
11 R. E. Palermo, P. P. Power and R. H. Holm, *Inorg. Chem.*, 1982, **21**, 173.
12 R. E. Palermo, R. Singh, J. K. Bashkin and R. H. Holm, *J. Am. Chem. Soc.*, 1984, **106**, 2600.
13 J. Cambray, R. W. Lane, A. G. Wedd, R. W. Johnson and R. H. Holm, *Inorg. Chem.*, 1977, **16**, 2565.

Proportion of C_2H_4 =

$$\frac{k_5K_0[Fe_4HS_2(SH)_2(SPh)_3]_e[C_2H_2]}{k_5K_0[Fe_4HS_2(SH)_2(SPh)_3]_e[C_2H_2] + k_6K_0[Fe_4HS_2(SH)_2(SPh)_3]_e[C_2H_2] + k_4[Fe_4HS_2(SH)_2(SPh)_3]_e} \quad (A4)$$

Proportion of H_2 =

$$\frac{k_4[Fe_4HS_2(SH)_2(SPh)_3]_e + k_6K_0[Fe_4HS_2(SH)_2(SPh)_3]_e[C_2H_2]}{k_5K_0[Fe_4HS_2(SH)_2(SPh)_3]_e[C_2H_2] + k_6K_0[Fe_4HS_2(SH)_2(SPh)_3]_e[C_2H_2] + k_4[Fe_4HS_2(SH)_2(SPh)_3]_e} \quad (A5)$$

14 K. S. Hagen, A. D. Watson and R. H. Holm, *Inorg. Chem.*, 1984, **23**, 2984.
15 G. B. Wong, M. A. Bobrik and R. H. Holm, *Inorg. Chem.*, 1978, **17**, 578.
16 R. H. Holm, *Chem. Soc. Rev.*, 1981, **10**, 455 and refs. therein.
17 E. J. Laskowski, R. B. Frankel, W. O. Gillum, G. C. Papaefthymiou, J. Renauld, J. A. Ibers and R. H. Holm, *J. Am. Chem. Soc.*, 1978, **100**, 5322.
18 R. A. Henderson and K. E. Oglieve, *J. Chem. Soc.*, *Dalton Trans.*, 1998, 1731.
19 K. L. C. Grönberg and R. A. Henderson, *J. Chem. Soc.*, *Dalton Trans.*, 1996, 3667 and refs. therein.
20 R. A. Henderson and K. E. Oglieve, *J. Chem. Soc.*, *Dalton Trans.*, 1993, 1467.
21 K. Izutsu, *Acid-Base Dissociation Constants in Dipolar Aprotic Solvents*, Blackwell, Oxford, 1990, ch. 2.
22 J. G. Reynolds, C. L. Coyle and R. H. Holm, *J. Am. Chem. Soc.*, 1980, **102**, 4350.
23 K. Tanaka, M. Nakamoto, M. Tsunomori and T. Tanaka, *Chem. Lett.*, 1987, 613.
24 R. A. Henderson, D. J. Lowe and P. Salisbury, *J. Organomet. Chem.*, 1995, **489**, C22.
25 R. A. Henderson, *Angew. Chem.*, 1996, **35**, 946 and refs. therein.
26 B. V. Pamphilis, B. A. Averill, T. Herskovitz, L. Que jnr. and R. H. Holm, *J. Am. Chem. Soc.*, 1974, **96**, 4159.
27 J. R. Dilworth, R. A. Henderson, P. Dahlstrom, T. Nicholson and J. A. Zubieta, *J. Chem. Soc.*, *Dalton Trans.*, 1987, 529.
28 R. A. Henderson and K. E. Oglieve, *J. Chem. Soc.*, *Dalton Trans.*, 1993, 1473 and refs. therein.
29 R. A. Henderson, *J. Chem. Soc.*, *Dalton Trans.*, 1982, 917.
30 R. G. Wilkins, *Kinetics and Mechanism of Reactions of Transition Metal Complexes*, VCH, Weinheim, 1991, ch. 1.

Paper 8/03223H